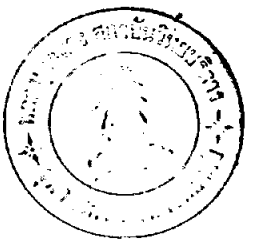

CHAPTER 3

EXPERIMENTAL AND PRELIMINARY INVESTIGATION

3.1 Preparation[9]

Single crystals of $CoWO_4$ were grown from a melt of 60 mole percent of an equimolar mixture of Na_2WO_4 and WO_3 and 40 mole percent of CoO. The mixture was melted together in a platinum crucible at 1050°C for 2 hours. The melts were cooled at the rate of 10°C per hour to 700°C after which it was left in the furnace to cool slowly to room temperature. The $Na_2W_2O_7$ was removed from the solidified melt by washing with concentrated sodium hydroxide solution to convert water insoluble $Na_2W_2O_7$ to soluble Na_2WO_4. The mixture was then filtered and washed with distilled water until free of alkali. The resulted dark blue transparent crystals were flat needle-shaped with the needle axis coinciding with the c crystallographic axis.

3.2 Chemical analysis[10]

The compound prepared as described in section 3.1 was mixed with a mixture of equal parts of Na_2CO_3 and K_2CO_3. The mixture was heated in a porcelain crucible for 10-15 minutes. After the melt was cooled, distilled water was added. The solution was boiled and filtered. The residue was kept to test for cobaltous ion, Co^{2+}.

The filtrate was acidified with dilute acetic acid, and evaporated to expel CO_2. The solution was divided into three parts and the test for the presence of the tungstate ion, $WO_4^{=}$, was carried out. Dilute HCl was added to the first portion. The white precipitate of hydrated tungstic acid $H_2WO_4.H_2O$ was produced at room temperature. Upon boiling it was converted to yellow tungstic acid H_2WO_4 which was insoluble in dilute acids. The second portion was treated with hydrochloric acid, a blue precipitate was produced after the addition of a little zinc. This was probably due to W_2O_5 or to WCl_5. The last portion was treated with $AgNO_3$ solution. The pale yellow precipitate of the ammonia soluble silver tungstate was obtained. It was decomposed by nitric acid with the formation of white hydrated tungstic acid. Hence it was confirmed that the filtrate was containing tungstate ion.

The residue from water extraction was dissolved in dilute HCl , boiled to expel CO_2 and then filtered. The filtrate was divided into three parts to test for cobaltous ion, Co^{2+}. Ammonia solution was added to the first portion. The blue basic salt was precipitated and readily soluble in excess ammonia. Concentrated HCl was added to the second portion, it was followed by the addition of solid NH_4SCN and amyl alcohol. After shaking, the blue color due to the cobalti-thiocyanate ion $\left[Co(SCN)_4\right]^{=}$ was passed into the alcohol layer. The third portion was neutralized with NaOH, acidified with acetic acid and then treated with solid potassium nitrite KNO_2. The yellow precipitate of potassium cobaltinitrite $K_3\left[Co(NO_2)_6\right].3H_2O$ was obtained. All of the tests mentioned above

confirmed the presence of the cobaltous ion.

Therefore, the compound was composed of Co^{2+} and $WO_4^{=}$. This indicated that this compound is $CoWO_4$ and was confirmed by an X-ray powder diffraction pattern described in section 3.5.1.

3.3 Density measurement

The density of $CoWO_4$ was measured by using the method of Archimedes[11]. $CoWO_4$ was weighed in air and then in water, since $CoWO_4$ is insoluble in water. From the apparent loss of weight the volume was computed and the density (ρ) was calculated from the formula

$$\rho = \frac{W \text{ in air}}{W \text{ in air} - W \text{ in water}} \quad \ldots\ldots\ldots 3.1$$

The density of $CoWO_4$ was found to be 7.75 ± 0.02 g/cm^3 at 28.0°C.

3.4 X-ray diffraction photographs of single crystals

A crystal which will be satisfactory in collecting X-ray diffraction data must be pure and possess a uniform internal structure which is called a single crystal. It should not be twinned. The phenomenon of twinning is the existence of two different orientations of a lattice in one crystal[12].

In order to obtain satisfactory single crystals, $CoWO_4$ crystals were first examined under a polarizing microscope. The suitable crystals appear uniformly transparent and uniformly dark

once for every 90^{o} rotated about the axis normal to crystal needle axis. The diffraction pattern of a suitable crystal should give the reflections which are single spots, and the pattern should be indexable in terms of a single three-dimensional lattice.

The single crystals of $CoWO_4$ used for structure determination are flat needle-shaped. One crystal of dimensions 0.009 x 0.028 x 0.058 mm. was mounted along the b axis and another of dimensions 0.009 x 0.027 x 0.098 mm. along the c axis.

3.4.1 Oscillation and rotation photographs

In the oscillation and rotation methods the single crystal is mounted along a selected axis on a goniometer head and the axis is set normal to the incident X-ray beam. If the crystal is rotated about this axis it is called the rotation method whereas the oscillation method requires that the crystal is oscillated within a certain angular range usually 10-15 degrees. The reflections are recorded on a cylindrical film whose axis coincides with the rotation axis. When the crystal is rotated or oscillated, the diffracted beam will form Laue cones which are coaxial with the rotation axis and will intersect the film in a set of circles which appear as straight lines when the film is flattened out (Figs. 3.1, 3.2) and these lines are called layer lines.

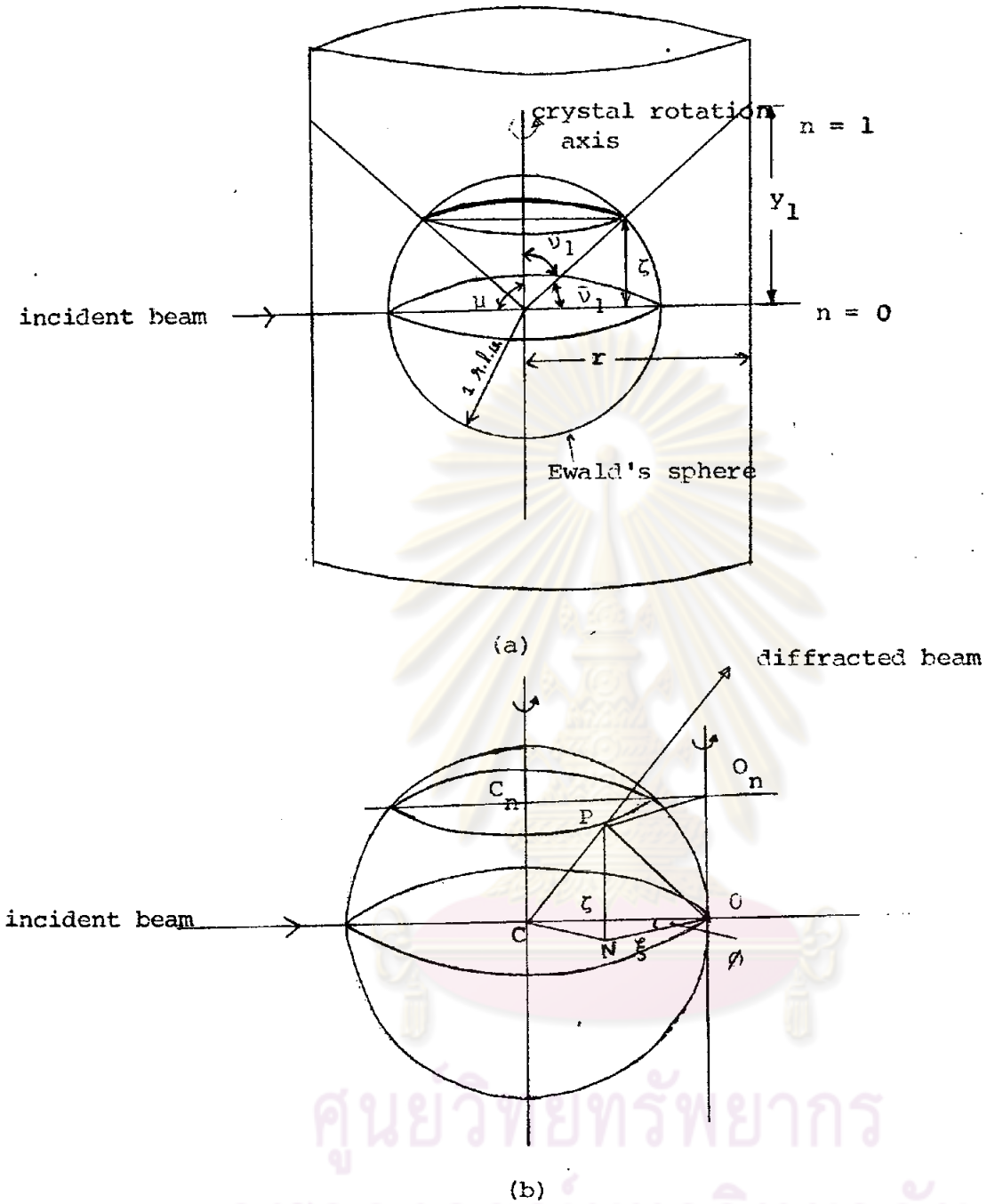

Fig. 3.1 (a) The rotating and oscillating crystal method.

(b) Showing the cylindrical reciprocal lattice coordinates.

Oscillation and rotation photographs are usually used to set a crystal rotation axis, to determine the cell edge along the rotation axis and to obtain preliminary information about crystal symmetry[7]. For setting the crystal rotation axis, the oscillation method is generally used rather than the rotation method because it gives a usable photograph in a shorter exposure time. However, after the crystal rotation axis has been correctly set, the rotation photograph should be made to check the crystal.

The cell edge along the rotation axis can be determined from the Laue equation

$$t \cos \nu_1 - t \cos \mu_1 = n\lambda \quad \ldots\ldots\ldots \quad 3.2$$

where t is the lattice constant along the rotation axis, ν is the angle between the diffracted X-ray beam and the rotation axis, μ is the corresponding angle for the incident beam, n is an integer and λ is the wavelength of the X-ray beam. For $\mu = 90^0$,

$$t \cos \nu_1 = n\lambda$$

$$\cos \nu_1 = n\frac{\lambda}{t} \quad \ldots\ldots\ldots \quad 3.3$$

Fig. 3.1 shows that y_1, the height of the first layer (n = 1) is given by

$$\tan \bar{\nu}_1 = \frac{y_1}{r} \quad \ldots\ldots\ldots \quad 3.4$$

where $\bar{\nu}_1 = 90 - \nu_1$. In terms of $\bar{\nu}_1$, eq.(3.3) becomes

$$\sin \bar{\nu}_1 = \frac{\lambda}{t} = \zeta_1 \quad \ldots\ldots\ldots \quad 3.5$$

$$t = \frac{\lambda}{\sin \bar{\nu}_1}$$

$$= \frac{\lambda}{\sin(\tan^{-1} y_1/r)} \quad \ldots\ldots\ldots 3.6$$

Similarly for the n th layer line

$$t = \frac{n\lambda}{\sin(\tan^{-1} y_n/r)} \quad \ldots\ldots 3.7$$

In this experiment a **Nonius** Weissenberg camera of diameter 57.3 mm. was used. The crystal was mounted along b as rotation axis. The axis was first set normal to the beam by using 20° oscillation photographs taken with Mo-radiation. The 280° oscillation photograph taken with Zr-filtered MoKα-radiation ($\lambda K\alpha$ = 0.71068 Å) was used to determine the cell parameter b. This is shown in Fig. 3.2(a) and the data are shown in Table 3.1 .

For the crystal mounted along c as rotation axis, the Unicam rotation and oscillation camera was used. The diameter of this camera is 60 mm. The axis was first correctly set by taking 15° oscillation photographs. The rotation photograph used for measurement the cell edge was taken with Ni-filtered CuKα-radiation ($\lambda K\alpha$ = 1.5418 Å). This is shown in Fig. 3.2(b) and the data are shown in Table 3.2 .

The X-ray tubes, Mo-target was run at 50 KV, 14 mA and Cu-target at 34 KV, 21 mA throughout the experiment.

Fig. 3.2(a) Oscillation photograph of $CoWO_4$, [010] as rotation axis, MoKα-radiation.

(b) Rotation photograph of $CoWO_4$, [001] as rotation axis, CuKα-radiation.

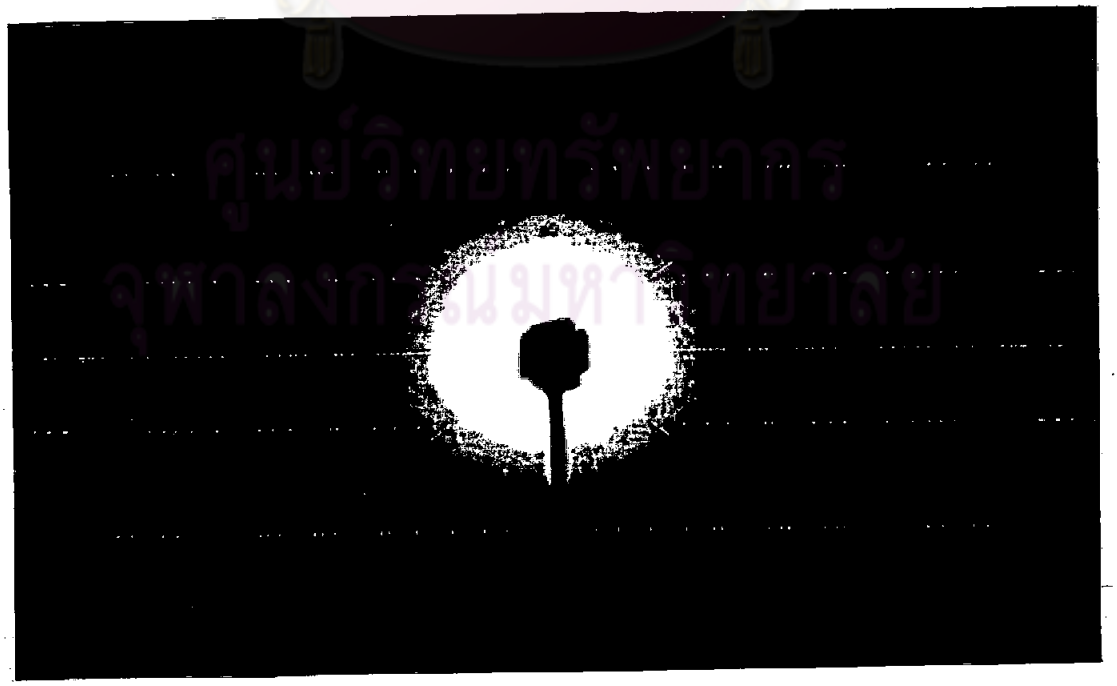

Table 3.1 Determination of the lattice constant, b, from [010] oscillation photograph, 2r = 57.3 mm., λ = 0.71068 Å.

layer	2Y mm.	$\tan\bar{\nu} = \frac{2y}{2r}$	$\bar{\nu}$ degree	$\zeta = \sin\bar{\nu}$	$b = \frac{n\lambda}{\sin\bar{\nu}}$ Å
1	7.25	0.1265	7.21	0.1255	5.66
2	14.85	0.2592	14.53	0.2509	5.67
3	23.20	0.4049	22.04	0.3753	5.68
4	33.10	0.5777	30.02	0.5003	5.68
5	45.90	0.8010	38.69	0.6251	5.68
6	64.75	1.1300	48.49	0.7488	5.69
					$b_{ave.}$=5.68

Table 3.2 Determination of the lattice constaht, c, from [001] rotation photograph, 2r = 60.0 mm., λ = 1.5418 Å.

layer	2z mm.	$\tan\bar{\nu} = \frac{2z}{2r}$	$\bar{\nu}$ degree	$\zeta = \sin\bar{\nu}$	$c = \frac{n\lambda}{\sin\bar{\nu}}$ Å
1	19.7	0.3283	18.18	0.3120	4.94
2	47.8	0.7967	38.54	0.6231	4.95
					$c_{ave.}$ = 4.95

3.4.2 Weissenberg photographs

The oscillation and rotation methods fail to complete the crystal structure analysis because the indexing of reflections is ambiguous and is very tedious. K. Weissenberg recognized this problem and devised a new recording method which is known as the Weissenberg method. The basis of the Weissenberg method is similar to that of the oscillation method except that only one selected cone is allowed to reach the film by using a cylindrical layer line screen to screen out unwanted cones (Fig. 3.3), and the film is made to translate synchronously with the oscillation of the crystal. The result of this is to spread the diffraction spots of the layer line over the two-dimensions of the film. A Weissenberg photograph gives two cell constants, the angle between them and the indicies of reflections and symmetry.

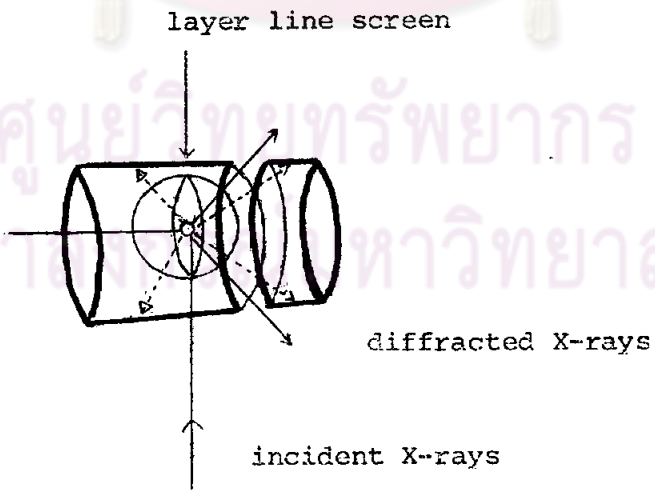

Fig. 3.3 The Weissenberg layer line screen.

For zero layer Weissenberg photograph, the incident X-ray beam is normal to the rotation axis and only zero layer line is allowed to reach the film. For upper layers the equi-inclination method is used. In this case the incident beam is inclined from the normal beam position at an angle μ_n, while the diffracted beam inclined at the same angle from the normal beam direction (Fig. 3.4). The angle μ_n is called the inclination angle of n th layer.

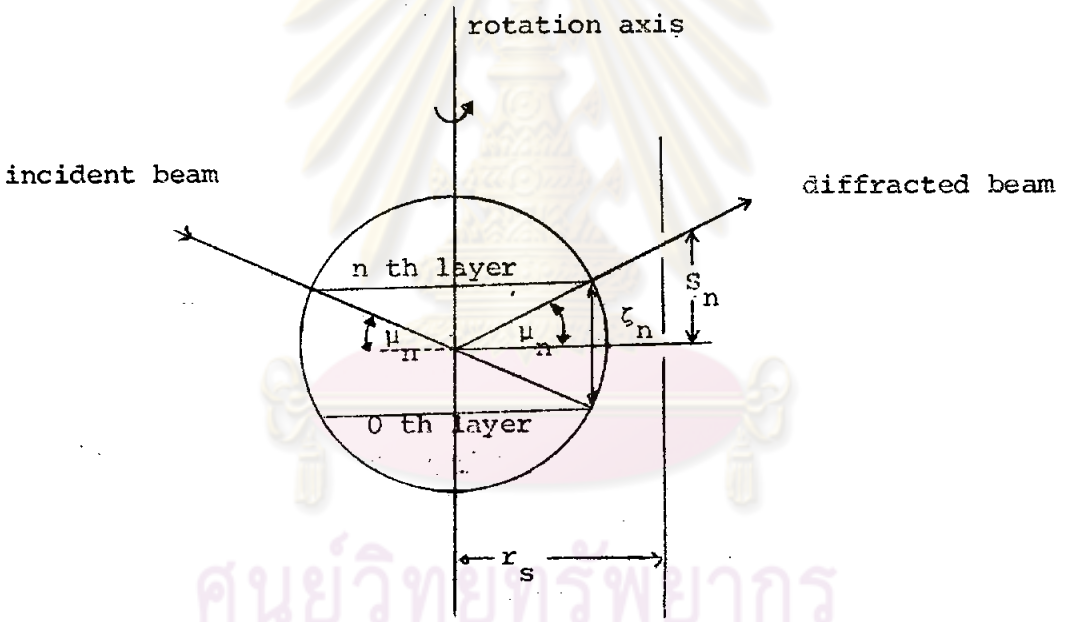

Fig. 3.4 Equi-inclination geometry for n th layer Weissenberg photograph.

The proper value of μ_n can be determined from Fig. 3.4

$$\mu_n = \sin^{-1}(\frac{\zeta_n}{2}) \quad \ldots\ldots\ldots\ldots \quad 3.8$$

where ζ_n can be obtained from the oscillation or rotation photographs. From eq.(3.5)

$$\zeta_n = \frac{n\lambda}{t} \quad \ldots\ldots\ldots\ldots \quad 3.9$$

Then

$$\mu_n = \sin^{-1}\frac{n\lambda}{2t} \quad \ldots\ldots\ldots\ldots \quad 3.10$$

The layer line screen must be shifted from its zero layer position, let it be S_n mm. It can be seen from Fig. 3.4 that

$$S_n = r_S \tan \mu_n \quad \ldots\ldots\ldots\ldots \quad 3.11$$

where r_S is the radius of the layer line screen. The slit's width of the layer line screen is usually adjustable. In practice the width is about 1.5 mm.

For intensity-data collection and space group determination, a Nonius Weissenberg camera of 57.3 mm. diameter was used with Zr-filtered MoKα-radiation ($\lambda K\alpha$ = 0.71068 Å). Weissenberg photographs using multiple-film technique with thin iron foils between successive films were taken:

1. [010] as rotation axis for h0l to h2l and $\bar{h}0l$ to $\bar{h}2l$ (Fig. 3.5). The necessary parameters for taking these photographs are listed in Table 3.3.

2. [001] as rotation axis for hk0 to hk3 (Fig. 3.6). The necessary parameters for taking these photographs are listed in Table 3.4.

The cylindrical reciprocal lattice coordinates of reflection spots, ξ , $\emptyset$ were obtained directly from measurement on the film. The reciprocal lattice nets were constructed as shown in Fig. 3.7 for [010] as rotation axis and Fig. 3.8 for [001] as rotation axis.

From [010] Weissenberg photographs, the reciprocal axes and the interaxial angles were obtained as follows

a^* = 0.152 r.l.u.

c^* = 0.144 r.l.u.

β^* = 90° .

[r.l.u. = reciprocal lattice unit]

From [001] Weissenberg photographs, the reciprocal axes and the interaxial angles were obtained as follows

a^* = 0.152 r.l.u.

b^* = 0.126 r.l.u.

γ^* = 90° .

Table 3.3 The necessary parameters for taking [010] Weissenberg photographs. The value of b was taken from Table 3.1 : b = 5.68Å, λ = 0.71068Å, r_s = 25.5 mm. .

n th layer	$\frac{n\lambda}{2b}$	$\mu_n = \sin^{-1} n\lambda/2b$	$\tan\mu_n$	$S_n = r_s \tan\mu_n$ mm.
1	0.0626	3.58	0.0626	1.60
2	0.1251	7.18	0.1260	3.21

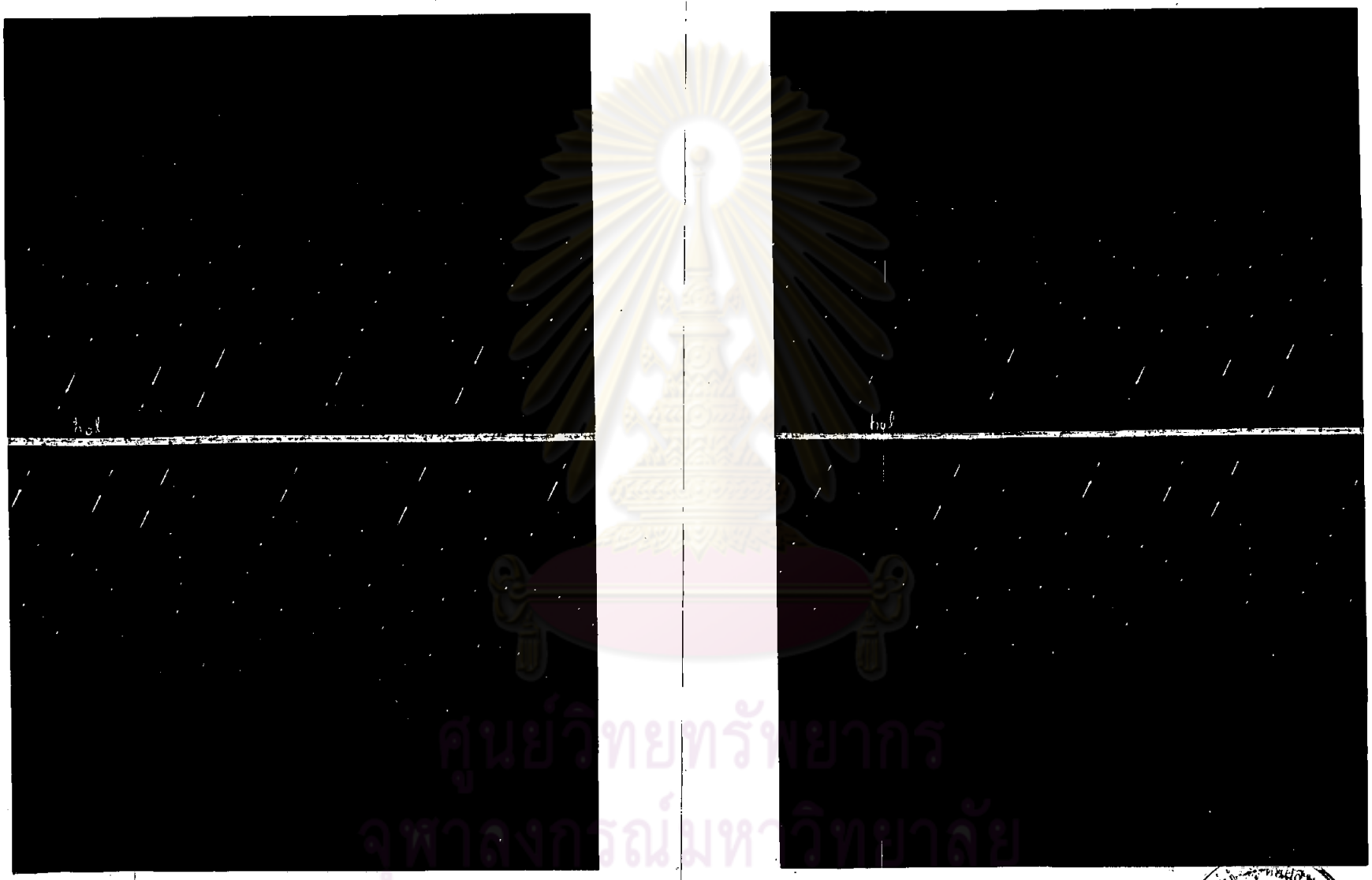

Fig. 3.5 [010] Weissenberg photograph of $CoWO_4$, MoKα-radiation

(a) 0 th layer ($\bar{h}$01)

(b) 0 th layer (h$\bar{0}$1)

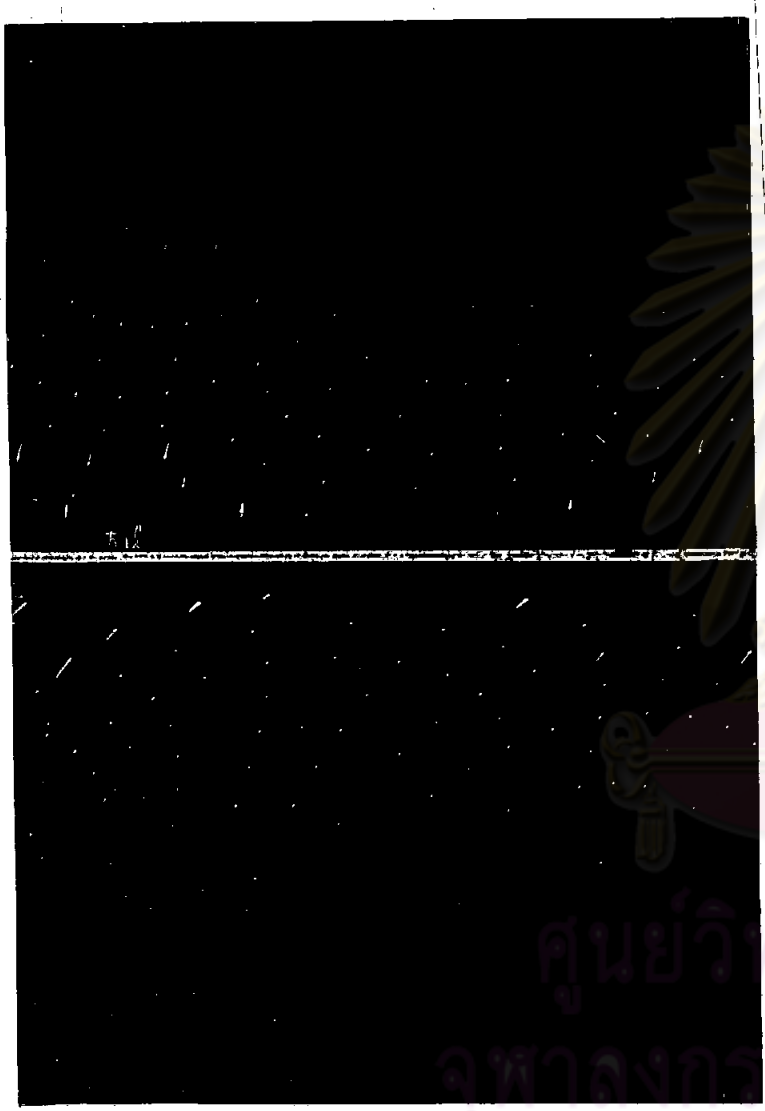

(c) 1 st layer ($\bar{h}11$)

(d) 1 st layer (h11)

(e) 2 nd layer (h21)

(f) 2 nd layer ($\bar{h}$21)

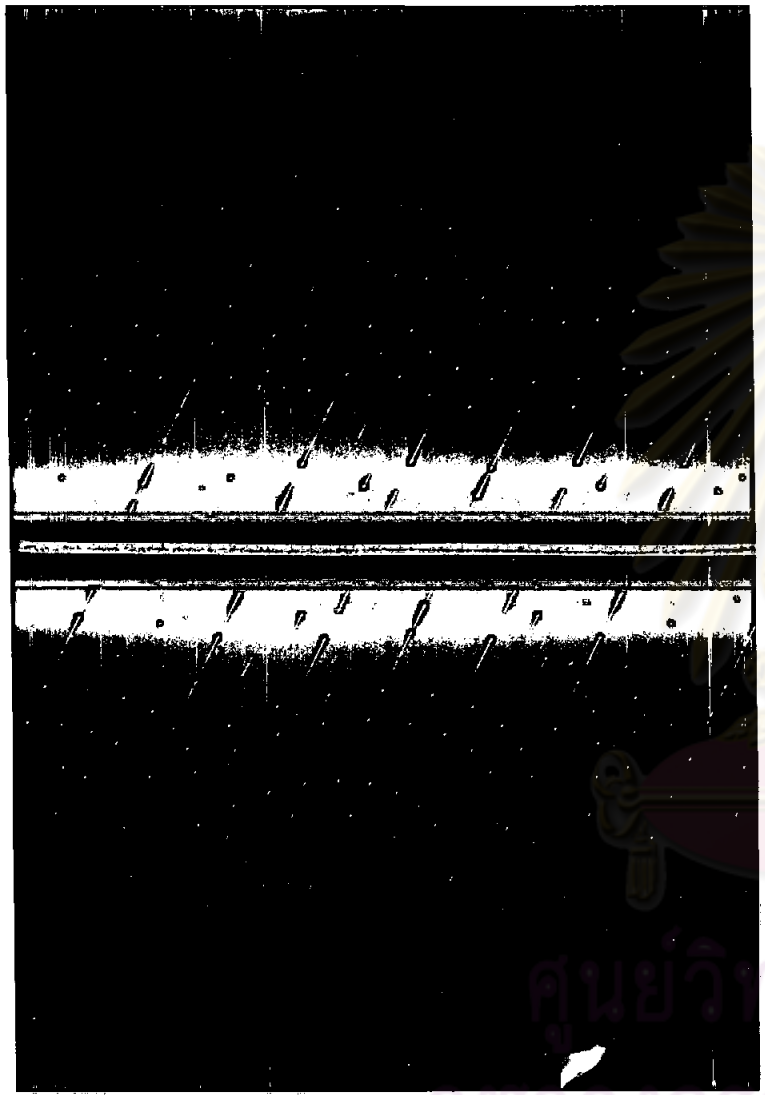

Fig 3.6 [001] Weissenberg photograph of $CoWO_4$ MoKα-radiation

(a) 0 th layer (hk0)

(b) 1 st layer (hkl)

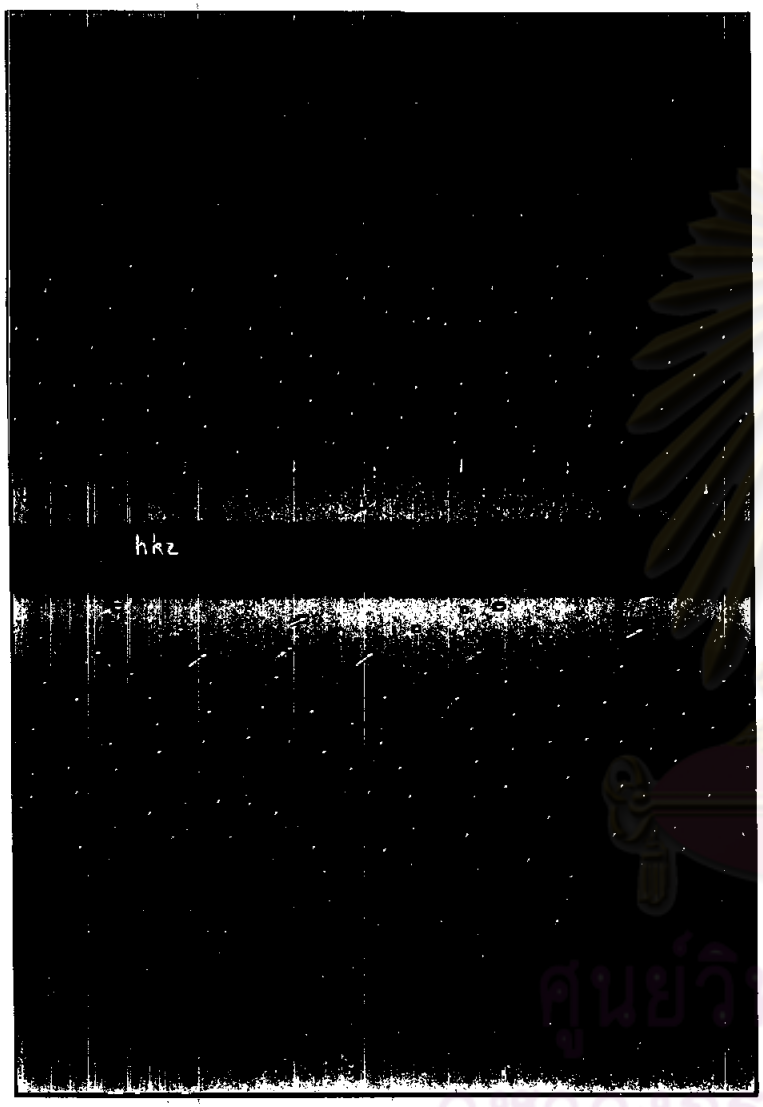

(c) 2 nd layer (hk2)

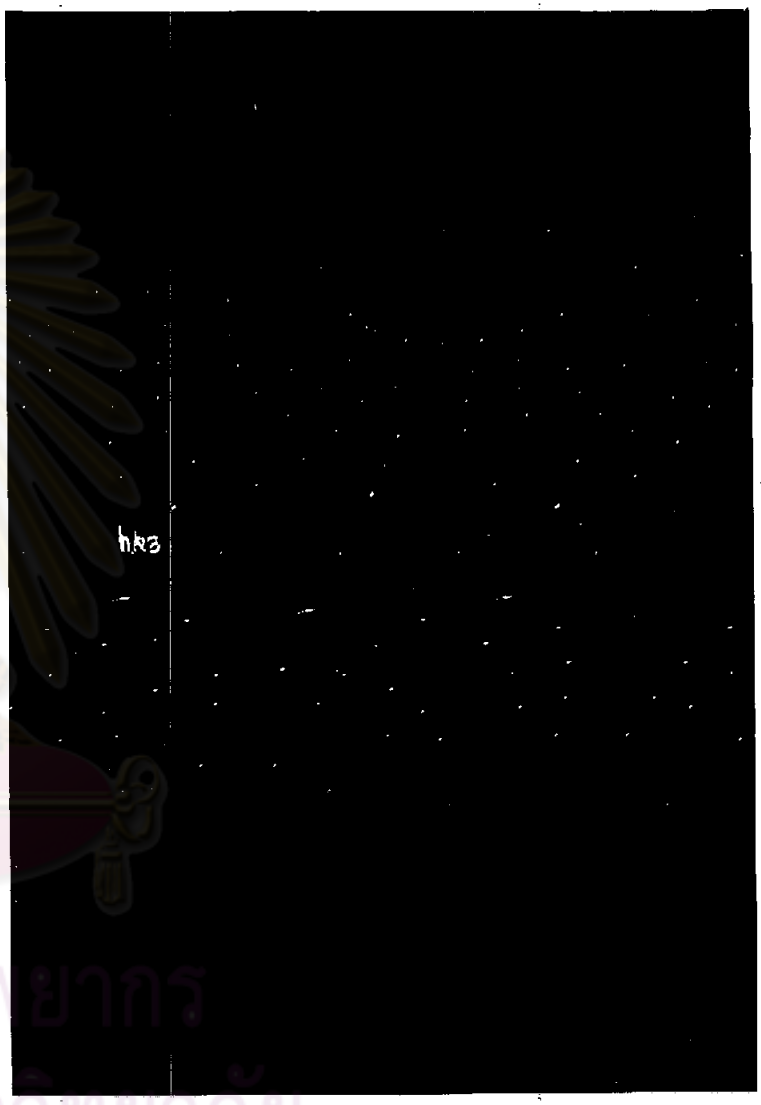

(d) 3 rd layer (hk3)

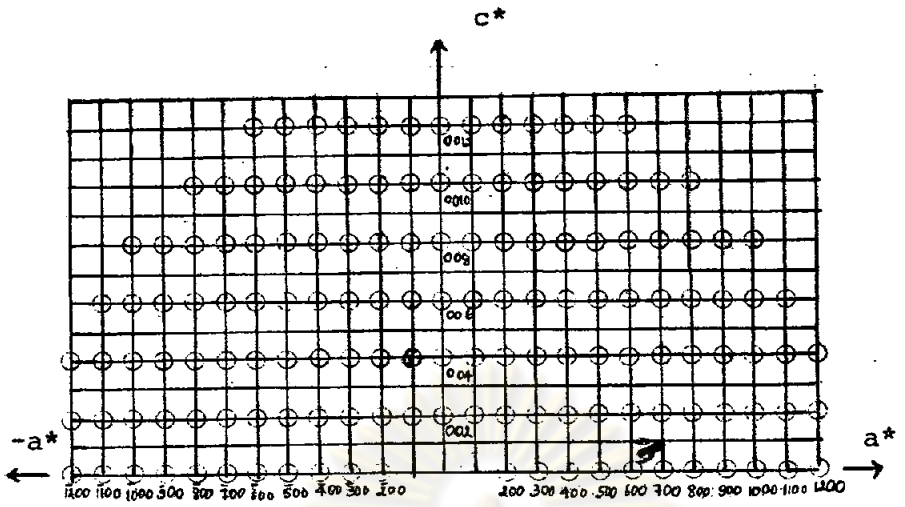

(a) 0 th layer

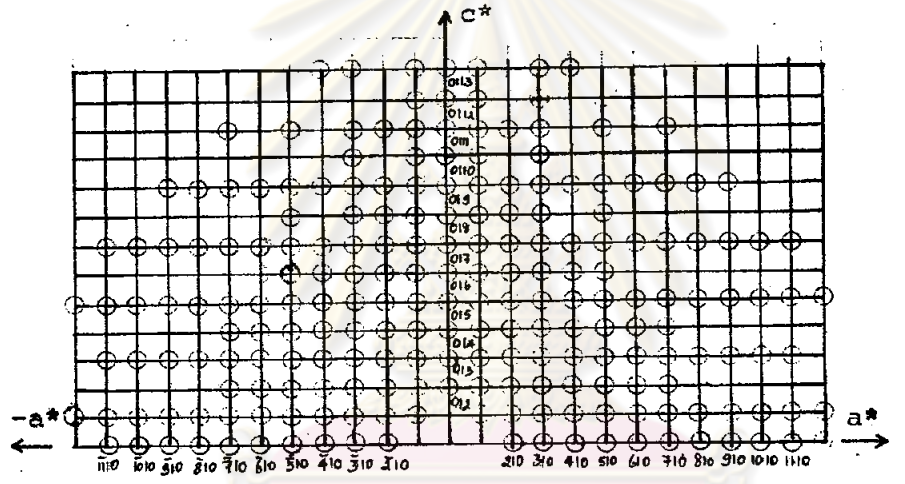

(b) 1 st layer

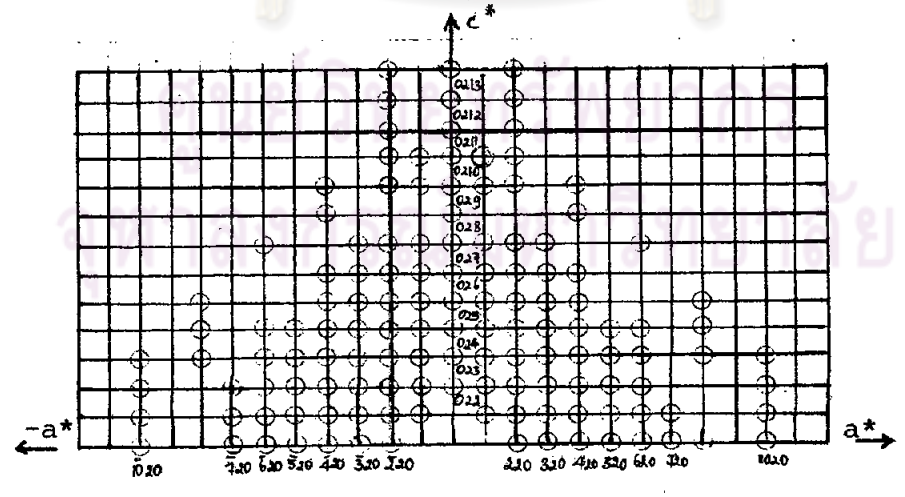

(c) 2 nd layer

Fig. 3.7 The reciprocal lattice nets, [010]as rotation axis.

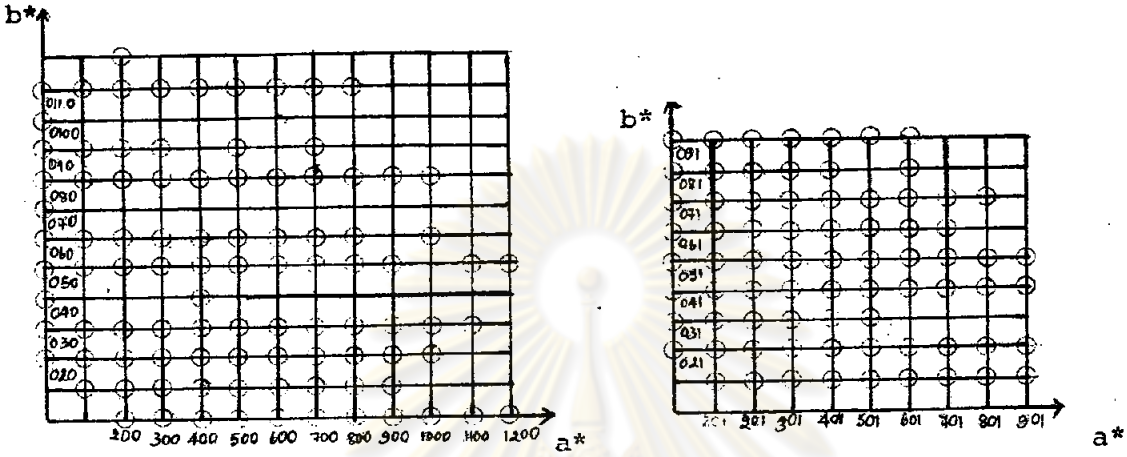

(a) 0 th layer

(b) 1 st layer

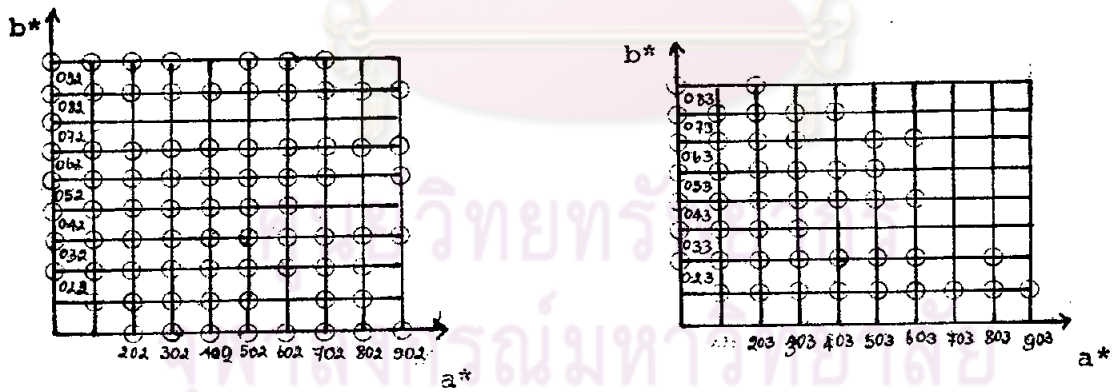

(c) 2 nd layer

(d) 3 rd layer

Fig. 3.8 The reciprocal lattice nets, [001] as rotation axis.

Table 3.4 The necessary parameters for taking [001] Weissenberg photographs. The value of c was taken from Table 3.2 : c = 4.95Å, λ = 0.71068 Å, r_s = 25.5 mm.

n th layer	$\frac{n\lambda}{2c}$	$\mu_n = \sin^{-1} n\lambda/2c$	$\tan\mu_n$	$S_n = r_s \tan\mu_n$ mm.
1	0.0718	4.12	0.0720	1.84
2	0.1436	8.25	0.1450	3.70
3	0.2154	12.43	0.2205	5.62

3.4.3 Determination of unit cell dimensions.

Preliminary unit cell dimensions of $CoWO_4$ were determined from oscillation, rotation and Weissenberg photographs. From Weissenberg photographs the reciprocal lattice constants were obtained.

The oscillation, Weissenberg and Laue photographs of $CoWO_4$ crystal show that there are a 2 fold axis lie along the b axis and the mirror plane perpendicular to it. These indicate that the Laue symmetry is 2/m and the crystal system is monoclinic. Therefore, the reciprocal lattice constants can be changed to the direct lattice by the formula

$$a = \frac{\lambda}{a^* \sin\beta^*}$$

$$b = \frac{\lambda}{b^*}$$

$$c = \frac{\lambda}{c^* \sin\beta^*}$$

$$\alpha = \gamma = \alpha^* = \gamma^* = 90^\circ$$

$$\beta = 180^\circ - \beta^*$$

The unit cell dimensions of $CoWO_4$ are shown in Table 3.5.

Table 3.5 Unit cell dimensions of $CoWO_4$.

reciprocal lattice	direct lattice
$a^* = 0.152$ r.l.u. $\alpha^* = 90^\circ$	$a = 4.68$ Å $\alpha = 90^\circ$
$b^* = 0.126$ r.l.u. $\beta^* = 90^\circ$	$b = 5.65$ Å $\beta = 90^\circ$
$c^* = 0.144$ r.l.u. $\gamma^* = 90^\circ$	$c = 4.94$ Å $\gamma = 90^\circ$
From Tables 3.1 and 3.2 : $b = 5.68$ Å, $c = 4.95$ Å	
Average cell dimensions $a = 4.68$ Å $\alpha = 90^\circ$ $b = 5.67$ Å $\beta = 90^\circ$ $c = 4.95$ Å $\gamma = 90^\circ$	

3.4.4 Intensity-data collection

For monoclinic crystal rotated about b axis, two blocks of data that need to be collected are hkl and $\bar{h}$kl.

In this work, multi-film equi-inclination Weissenberg technique was used to record intensities on layers h0l to h2l and $\bar{h}$0l to $\bar{h}$2l using MoKα-radiation. Every layer was exposed for 150, 100 and 10 hours using three films each time. For Weissenberg photographs of 150 and 100 hours exposure time, thin iron foils were placed between successive films, but for that of 10 hours exposure time, the film of thin silver foils were used. This technique was also used for hk0 data except that the exposure times were 130 and 90 hours instead, and the thin iron foils were used both times.

The intensity data of 550 independent reflections were obtained of which are 92 reflections for hk0 data and 458 reflections for h0l and $\bar{h}$0l to h2l and $\bar{h}$2l data.

3.4.5 Measurement of intensity by a microdensitometer

Intensities were measured by a Nonius microdensitometer using the screen with a small aperture of 0.5 mm.diameter.

The intensity of a reflection spot was determined as follows: the degree of blackening (I) of a reflection spot was measured and immediately afterwards the background blackness (I_o) surrounding the spot. The intensity were determined from the value of the

ratio I_o/I using the accompanying graph shown in Fig. 3.9. This graph is plotted between the values of D and n, where D is the density of the reflection and n is the number of times which a crystal was passed on a Weissenberg camera through a given reflection angle. The density is equal to log I_o/I and directly proportional to the intensity. Hence, the intensities measured are relative intensities.

The Nonius microdensitometer was calibrated with standard intensity scale of $CoWO_4$ before using in this experiment. The intensities of the standard intensity scale (I_S) and that measured by the Nonius microdensitometer (I_M) are compared in Table 3.6.

The X-radiation used for collecting data was MoKα which composed of $K\alpha_1$ and $K\alpha_2$ radiations, so the intensities recorded were the sum of these two wavelengths. The intensity of $K\alpha_1$ reflections are two times the $K\alpha_2$. For low values of $\sin\theta$ the reflections for $K\alpha_1$ and $K\alpha_2$ are not separated but for higher values of $\sin\theta$ these reflections are partially resolved, and becomes completely separated with sufficiently high values of $\sin\theta$. In the case of complete resolution, the intensity of $K\alpha_1$ was measured alone and multiplied by 1.5 to account for the absence of $K\alpha_2$. For partially resolved reflections the intensity of $K\alpha_1$ was also measured but the factor to be multiplied was obtained from the graph in Fig. 3.10. This graph was constructed by using the factor 1.0 for the reflection just before beginning of $K\alpha_1$, $K\alpha_2$ separation and the factor 1.5 for the reflection that is just completely separated to two reflections.

Table 3.6 The comparison of the intensities between the standard intensity scale (I_S) and that measured by the Nonius microdensitometer (I_M)

No.	I_S	I_M	$K=I_M/I_S$	No.	I_S	I_M	$K=I_M/I_S$
1	334	-	-	18	63	146.67	2.33
2	303	-	-	19	57	137.50	2.41
3	275	-	-	20	51	148.33	2.91
4	250	-	-	21	46	106.67	2.32
5	227	-	-	22	41	86.67	2.11
6	206	-	-	23	37	81.67	2.21
7	187	-	-	24	33	85.00	2.58
8	170	-	-	25	30	78.33	2.61
9	150	-	-	26	27	78.33	2.90
10	140	260.00	1.86	27	24	74.00	3.08
11	127	247.50	1.95	28	21	51.67	2.46
12	115	231.67	2.01	29	19	45.00	2.37
13	104	217.50	2.09	30	17	28.33	1.67
14	94	214.17	2.28	31	15	35.00	2.33
15	85	188.33	2.22	32	13	35.83	2.76
16	77	178.33	2.32	33	11	22.50	2.05
17	70	156.67	2.24				

$$K_{average} = \frac{56.07}{24} = 2.34$$

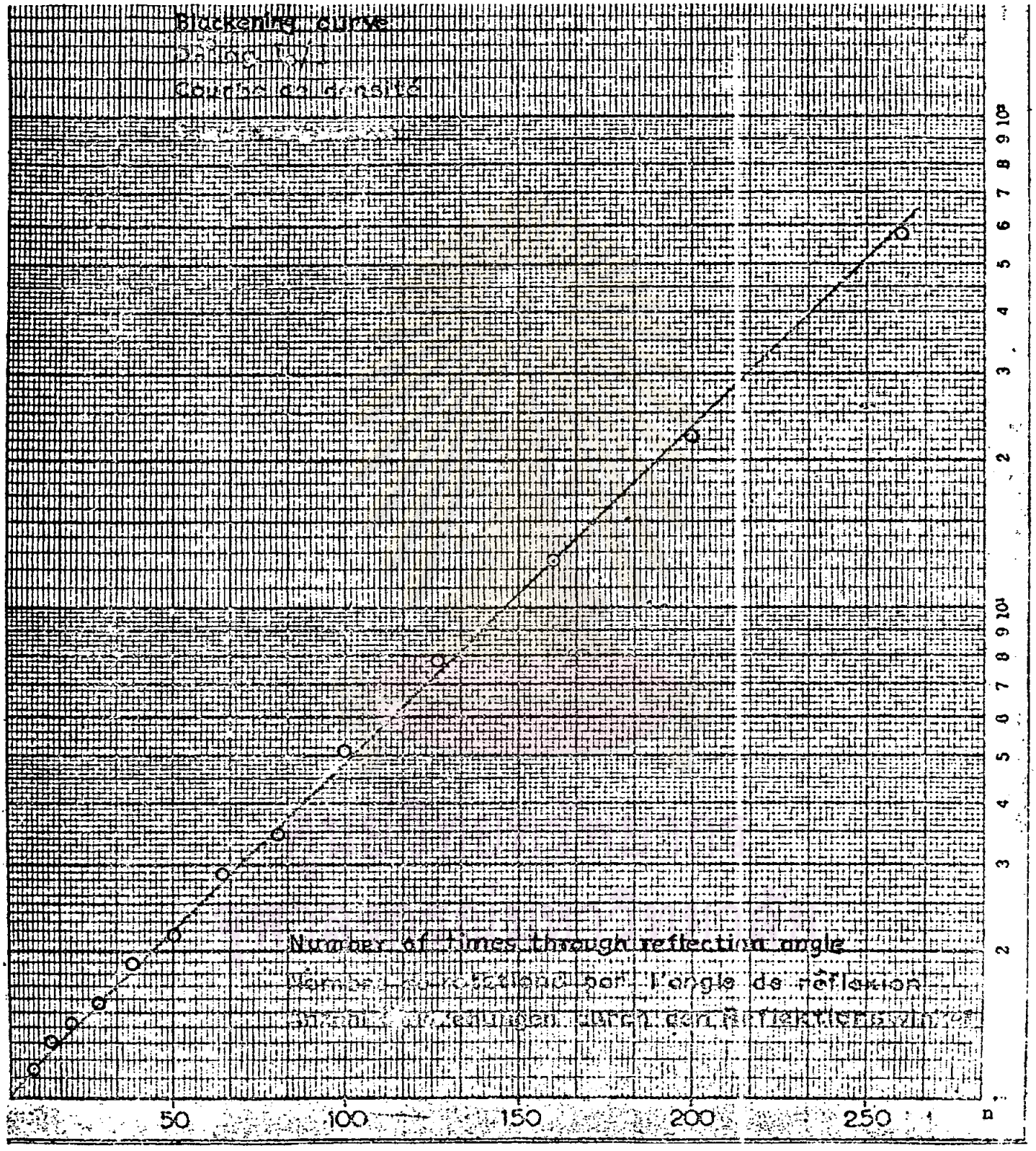

Fig. 3.9 The graph showing the relation between the values of D and n.

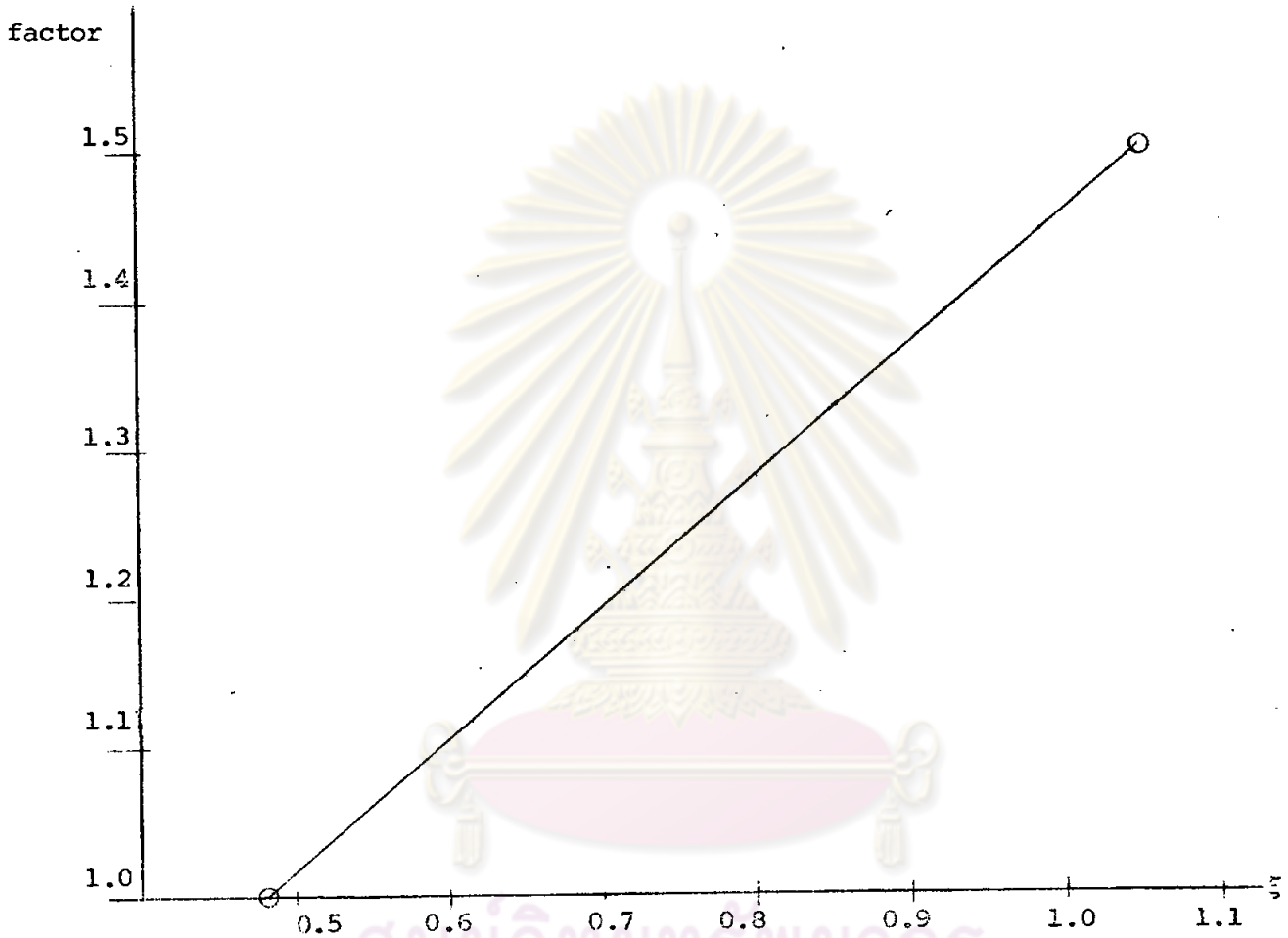

Fig. 3.10 The relation between the theoretical factor to correct the intensities due to $K\alpha_1$, $K\alpha_2$ separation and the value of ξ.

3.5 Powder photographs

The powder method makes use of a polycrystalline material oriented at random to a monochromatic X-ray beam[5]. The conditions for diffraction are similar to the rotation method. When a tiny crystal (about 10^{-3} mm. in diameter) in the sample is oriented so that a particular set of lattice planes makes the appropriate Bragg angleθ to the incident beam, the diffracted beam will make an angle 2θ with the undeviated beam as shown in Fig. 3.11(a). The identical lattice planes of other tiny crystals can be oriented at the same angle θ to the beam and send out the diffracted beam in the same angle 2θ around the incident direction. These diffracted beams will form a cone which is coaxial with the incident beam and has a half-apex angle 2θ (Fig. 3.11 (b)). Simultaneously, other lattice planes with different spacing satisfy the Bragg condition and generate reflection cones which are also coaxial with the incident beam but have different half-apex angles (Fig. 3.11(c)). The samples always rotate continuously during the exposure to ensure the existence of a sufficient number of the required orientation to give dense reflection cones.

The powder method provides much useful information. In the work reported here this method was used to identify the sample and to refine the unit cell parameters. The X-ray powder data for $CoWO_4$ were recorded at 26°C with the Guinier-Hägg XDC-700 focusing powder camera using $CuK\alpha_1$-radiation (λ = 1.54051 Å),

34 KV, 21 mA exposed for two hours. Silicon was used as the internal calibration standard. The photograph is shown in Fig. 3.12.

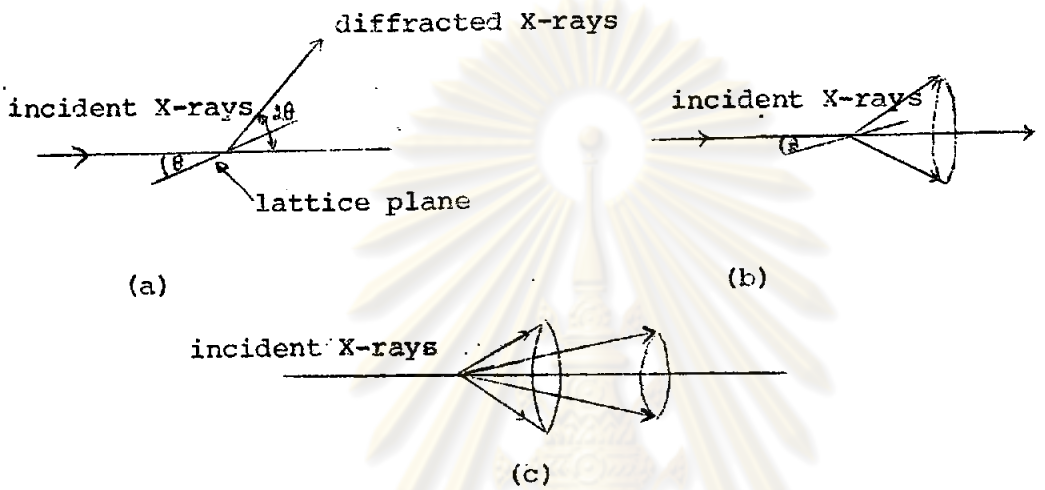

Fig. 3.11 (a) Bragg condition for diffraction.

(b) A cone of diffracted ray for the identical lattice planes.

(c) Cones of diffracted ray which have different half-apex angles.

Fig. 3.12 Powder photograph of $CoWO_4$ mixed with silicon, $CuK\alpha_1$-radiation, exposed 2 hours at 34 KV/21 mA.

3.5.1 Qualitative analysis by JCPDS* Powder Diffraction File

The principle of the identification of substance by X-ray powder diffraction is based on the fact that each crystalline substance produces its own characteristic pattern which is different from the pattern given by other substances.

The procedure for identifying a powder diffraction pattern consists of measuring the diffraction angles and the intensities, calculating the spacing, d of the reflecting planes, choosing the 3-8 strongest lines arranged in decreasing order of their relative intensities, and then using the JCPDS Powder Diffraction File to identify that compound[5,13]. The sequence for using the Powder Diffraction File is as follows. First, the correct Hanawalt group are searched for the strongest line; it may be necessary to consult two or three Hanawalt groups if the value of the strongest line close to the limit between them. Second, the second column in the appropriate Hanawalt group is taken into consideration to search for a match with the second strongest line. Third, the entry which also show a match for the third strongest line is selected and then the compound might be known. If there are two sets of entries which have d values that are reasonably close to the observed values, they may be distinguished via other data such as the relative intensities of the reflections. If the three strong-

---

*JCPDS = Joint Committee on Powder Diffraction Standards

est lines of a diffraction pattern do not lead to an identification, the sample may be a mixture of compounds.

The $CoWO_4$ compound prepared as described in section 3.1 was also identified by using the JCPDS Powder Diffraction File. The intensity of each diffraction line was measured with a Nonius microdensitometer. The values of S_o, S and $(S-S_o)$ were obtained from the Guinier film where S_o is the reading in mm. of the reference primary line and S is the reading in mm.of each diffraction line. From Table 3.7 the values of reflecting angles θ which correspond to $(S-S_o)$ of silicon were given. By using the graph plotted between $\theta/(S-S_o)$ and $(S-S_o)$ of silicon (Fig. 3.13), the values of $\theta/(S-S_o)$ and θ for each reflection were obtained[14]. From Bragg's equation the values of d_{hkl} were calculated and they were then identified by the Powder Diffraction File. The results indicated that this compound is $CoWO_4$. The values for these calculations are listed in Table 3.8.

Table 3.7 Calculated silicon data for copper ($CuK\alpha_1$) radiation.

hkl	θ^o	$(S-S_o)_{calc.}$ mm.
111	14.2214	49.725
220	23.6517	82.698
311	28.0616	98.117
400	34.5655	120.858
331	38.1887	133.527
422	44.0158	153.901

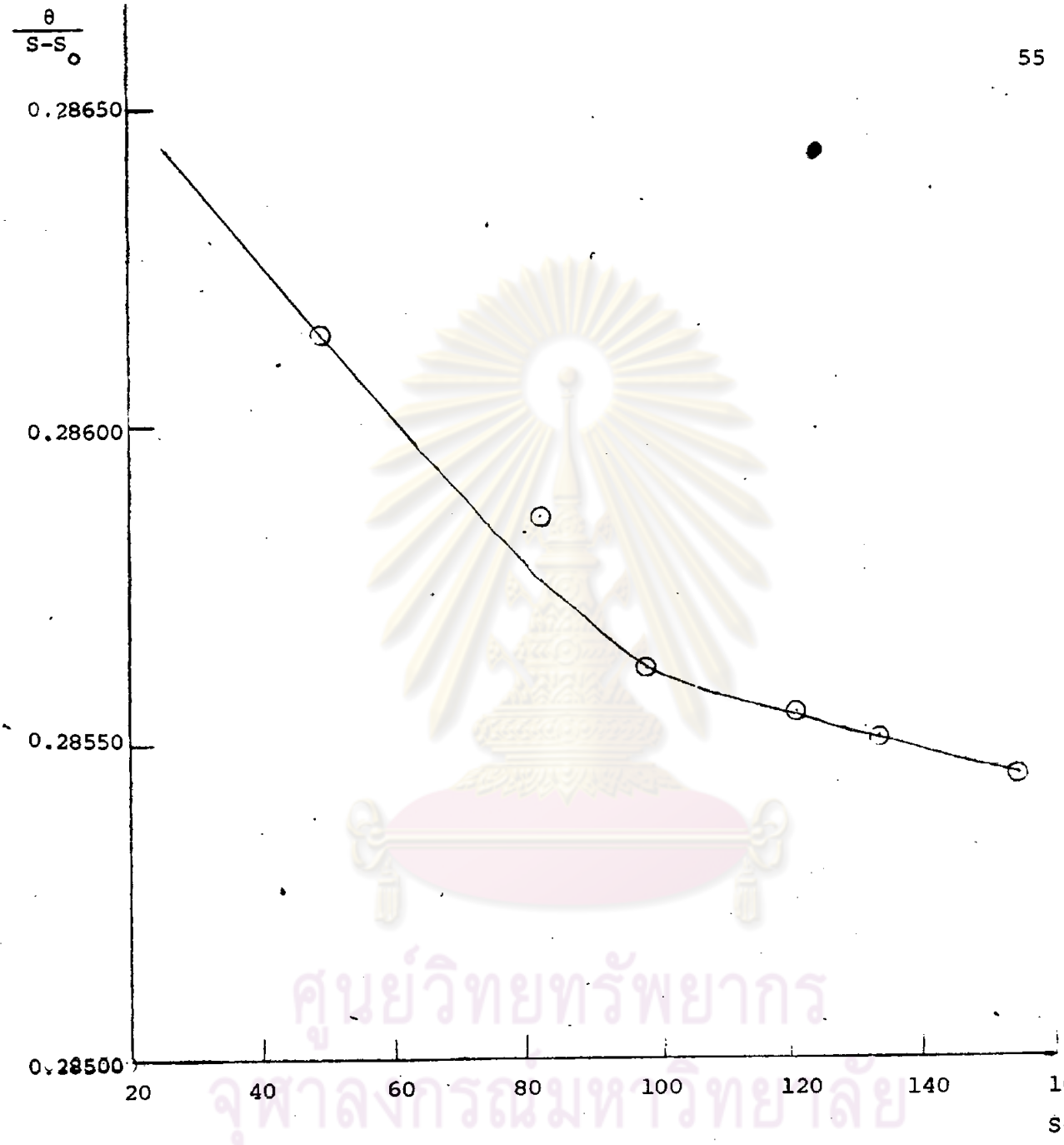

Fig. 3.13 The graph plotted between $\theta/(S-S_o)$ and $(S-S_o)$ of silicon.

Table 3.8 (a) The powder data obtained from X-ray diffraction pattern of $CoWO_4$. S_o = 22.90 mm. , λ = 1.54051 Å

I/I_1	S mm.	$S-S_o$ mm.	θ degree	$\theta/(S-S_o)$	$d_o = \lambda/2\sin\theta_o$	$d_{ref.}$**
<	50.08	27.18	7.7846	.286410	5.689	5.683
30	56.00	33.10	9.4778	.286337	4.682	4.673
29	64.45	41.55	11.8929	.286233	3.737	3.733
29	65.91	43.01	12.3101	.286215	3.616	3.608
*	72.60	49.70	14.2214	.286145	-	-
100	76.40	53.50	15.3061	.286095	2.919	2.916
<	77.88	54.98	15.7286	.286078	2.841	2.842
22	86.32	63.42	18.1369	.285980	2.474	2.473
21	86.60	63.70	18.2161	.285978	2.464	2.464
<	87.55	64.65	18.4858	.285967	2.429	2.428
12	90.30	67.40	19,2722	.285937	2.334	2.335
<	95.04	72.14	20.6237	.285885	2.188	2.185
<	95.25	72.35	20.6835	.285881	2.181	2.180
10	100.50	77.60	22.1803	.285828	2.040	2.041
<	102.98	80.08	22.8868	.285800	1.981	1.979
*	105.64	82.74	23.6517	.285856	-	-
<	108.21	85.31	24.3767	.285742	1.866	1.866
<	111.34	88.44	25.2679	.285707	1.805	1.803

Table 3.8 (a) (continued)

I/I_1	S mm.	$S-S_o$ mm.	θ degree	$\theta/(S-S_o)$	$d_o = \lambda/2\sin\theta_o$	$d_{ref.}$**
14	114.00	91.10	26.0255	.285681	1.755	1.755
<	115.20	92.30	26.3673	.285670	1.734	1.733
25	117.23	94.33	26.9456	.285652	1.700	1.698
23	117.45	94.55	27.0081	.285649	1.696	1.695
*	121.15	98.25	28.0616	.285614	-	-
<	124.72	101.82	29.0793	.285595	1.585	1.583
16	131.10	108.20	30.8995	.285578	1.500	1.500
<	134.55	111.65	31.8841	.285572	1.458	1.457
<	136.22	113.32	32.3606	.285568	1.440	1.436
<	136.86	113.96	32.5430	.285565	1.432	1.432
<	137.25	114.35	32.6542	.285564	1.428	1.426
<	143.20	120.30	34.3517	.285550	1.365	1.365
*	143.95	121.05	34.5655	.285547	-	-
<	148.21	125.31	35.8114	.285532	1.316	1.316
<	148.90	126.00	35.9768	.285530	1.311	1.311
<	151.91	129.01	36.8345	.285517	1.285	1.283
<	154.30	131.40	37.5158	.285508	1.265	1.264
*	156.66	133.76	38.1887	.285502	-	-
<	163.32	140.42	40.0867	.285477	1.196	-
<	165.74	142.84	40.7765	.285470	1.179	-

Table 3.8 (a) (continued)

I/I_1	S mm.	$S-S_o$ mm,	θ degree	$\theta/(S-S_o)$	$d_o = \lambda/2\sin\theta_o$	$d_{ref.}$**
<	167.30	144.40	41.2212	.285465	1.169	-
*	177.10	154.20	44.0158	.285446	-	-

< = less than 10

* = silicon line

$d_{ref.}$** obtained from the JCPDS data card No. 15-867.

Table 3.8 (b) The values of d_o and $d_{ref.}$ of the three strongest lines.

$(I/I_1)_o$	d_o	$d_{ref.}$	$(I/I_1)_{ref.}$
100	2.919	2.916	100
30	4.682	4.673	30
29	3.737	3.733	30

3.5.2 Accurate unit cell dimensions

The unit cell dimensions of $CoWO_4$ were refined by using CELNE program written by J. Tegenfeldt and N-O Ersson, Institute of Chemistry, University of Uppsala, Sweden, and modified for NEAC computer by Crystallography Group, Department of Physics, Chulalongkorn University, under the supervision of R. Liminga, Institute of Chemistry, University of Uppsala, Sweden. The method of least squares was used in the refinement.

The data used for the refinement were 30 observed $\sin^2\theta_{hkl}$ and the Miller indicies hkl. The Miller indicies were obtained by indexing the diffraction lines using the formula for monoclinic crystal with b unique axis[15]:

$$\sin^2\theta_{hkl} = Ah^2 + Bk^2 + Cl^2 - Dhl$$

where

$$A = \frac{\lambda^2}{4a^2 \sin^2\beta}$$

$$B = \frac{\lambda}{4b^2}$$

$$C = \frac{\lambda^2}{4c^2 \sin^2\beta}$$

$$D = \frac{\lambda^2}{2ac \sin^2\beta}$$

The values of a, b, c and β were obtained from Table 3.5. The results of refinement are shown in Table 3.9.

Table 3.9 Powder diffraction data for $CoWO_4$.

hkl	$\sin^2\theta_o \times 10^5$	$\sin^2\theta_c \times 10^5$	d_o Å	I/I_1
010	1835	1836	5.689	<
100	2711	2711	4.682	30
011	4247	4258	3.737	29
110	4545	4547	3.616	29
111	6968	6973	2.919	100
020	7348	7345	2.841	<
002	9690	9689	2.474	22
021	9772	9767	2.464	21
120	10054	10056	2.429	<
200	10844	10843	2.334	12
102	12407	12407	2.188	<
121	12476	12482	2.181	<
112	14252	14243	2.040	10
211	15124	15109	1.981	<
022	17035	17034	1.866	<
220	18220	18188	1.805	<
130	19221	19237	1.755	14
122	19724	19752	1.734	<
202	20535	20547	1.700	25

Table 3.9 (Continued)

hkl	$\sin^2\theta_o \times 10^5$	$\sin^2\theta_c \times 10^5$	d_o Å	I/I_1
221	20622	20618	1.696	23
013	23621	23636	1.585	<
113	26371	26358	1.500	16
222	27900	27892	1.458	<
311	28649	28667	1.440	<
132	28937	28933	1.432	<
023	29113*	29144	1.428	<
123	31841*	31867	1.365	<
041		31802		
321	34236*	34176	1.316	<
141	34511	34517	1.311	<
312	35942	35946	1.285	<
232	37086	37074	1.265	<
322	41467	41454	1.196	<
241	42655	42653	1.179	<
114	43424*	43317	1.169	<

* Reflections not used in the least squares refinement.

< = less than 10

The final cell parameters obtained were : a = 4.678 $\pm$ 0.001, b = 5.684 $\pm$ 0.001, c = 4.949 $\pm$ 0.001 Å; β = 90.04 $\pm$ 0.03^{0} ; V = 131.610 Å^{3}.

3.5.3 Number of formula unit per cell

The number of formula unit per cell were calculated from the formula

$$Z = \frac{D_{obs.} \times V \times N}{M}$$

where Z = the number of formula unit per cell

$D_{obs.}$ = observed density = 7.75 g/cm^{3}

V = cell volume = 131.610 x 10^{-24} cm^{3}

N = Avogadro's number = 6.02 x 10^{23}

M = Molecular weight = 306.779 atomic mass unit

The value of calculated Z is 2.001 . However, Z must be an integer, so Z = 2 and the calculated density = 7.744 g/cm^{3}.

3.6 Space group

Figs. 3.7, 3.8 and Table 3.10 show that the conditions for the systematic presence of reflections correspond to two possible space groups Pc and P2/c.

Table 3.10 Conditions for the systematic presence of reflections of $CoWO_4$ crystal.

Reflections	Condition for systematic presence of reflections	Interpretation	Symbol
hkl	no condition	Primitive	P
h0l	l = 2n	Glide plane perpendicular to b, translation c/2	c
0k0	no condition	-	-

The reasons for the conclusion that the space group is probably P2/c are as follows: First, since the value of Z, number of formula unit per cell, equals to 2, the number of oxygen atoms in the unit cell must be 8. These might prefer position 4(g) of P2/c rather than 2(a) of Pc space group. Second, the Patterson map gives the position of tungsten atom in special position 2(e) of space group P2/c.

The space group P2/c was subsequently confirmed by structure analysis.